



Research article

Preparation, bacteriostatic, and *in silico* analysis of halogenated 4-methoxyphenyl-triazene derivatives

Davlye Noissy Diosing¹, Ainaa Nadiah Abd Halim^{*1}, Nor Hisam Zamakshshari¹, Zainab Ngaini¹, Yeo Kai Wei¹, Akshatha Handattu Shankaranarayana², and B. R. Prashantha Kumar²

¹Faculty of Resource Science and Technology, Universiti Malaysia Sarawak, 94300 Kota Samarahan, Sarawak, Malaysia

²Department of Pharmaceutical Chemistry, JSS College of Pharmacy, Sri Shivarathreeswara Nagar, Mysuru- 570015, India

*Corresponding author: ahanadiah@unimas.my

Received: 13 September 2024; Revised: 10 December 2024; Accepted: 3 December 2025; Published: 27 March 2025

Abstract

A series of diazoamino compounds, also known as triazene derivatives were successfully synthesised through the N-coupling diazotisation of *p*-anisidine with various halogenated substituted anilines at *ortho*, *meta*, and *para* positions. The series was obtained in low to moderate yields of 13-56%. Structural elucidation was performed via FTIR, ¹H, and ¹³C NMR techniques. With ampicillin served as a positive control, the antibacterial efficacy of the synthesised compounds against *Escherichia coli* ATCC 25922 and *Staphylococcus aureus* ATCC 25923 via the Kirby-Bauer disk diffusion resulted in moderate to good inhibition measuring 6.6 ± 0.25 to 10.0 ± 0.00 mm, respectively. The minimum inhibitory concentration (MIC) values indicating inhibition of ≥ 8.8 mm yielded promising results, with MICs ranging from 82 to 121 ppm for *E. coli* and from 87 to 101 ppm for *S. aureus*. These values exceeded the standard ampicillin range of 96 to 127 ppm, suggesting potential for broader clinical applications. Molecular docking analysis of the compounds against CrtM and MurE protein receptors further supported these findings with binding scores of -7.48 to -8.27 kcal/mol and -7.26 to -7.94 kcal/mol, respectively. Notably, these scores surpassed those of ampicillin, which scored only -7.23 kcal/mol and -6.92 kcal/mol, respectively. This enhanced activity is believed to be attributed to the presence of hydrogen bonding and other hydrophobic interactions. Additionally, the bioavailability competencies of all compounds tested via ADMET analysis demonstrated compliance of each compound with Lipinski's rule of five with zero violations.

Keywords: diazoamino, antibacterial activities, ADMET, N-coupling, *in silico*

Introduction

Nitrogen-based organic molecules, such as quinolones, pyrazole, and sulphadiazine, are prevalent in diverse areas, particularly in medicine. Although these nitrogen-containing heterocycles are beneficial for certain industrial and biological applications, they can exhibit toxicity due to their reactivity and interactions with biological targets [1]. In some cases, these compounds are susceptible to metabolic degradation, which limits their bioavailability [2] and therapeutic efficacy [3]. Concurrently, the issue of drug-resistant bacterial infection, commonly referred to as antimicrobial resistance (AMR), has been a constantly growing problem. According to the Institute for Health Metrics and Evaluation, drug-resistant issues caused up to 5 million fatalities in Malaysia alone in 2019, with AMR accounting for 1.3 million of those deaths. Furthermore, the latest data

reported by the Ministry of Health Malaysia and the Ministry of Agriculture and Food Security in the MyAP-AMR 2022-2026, indicate that the resistance rate of *Escherichia coli* in urinary tract infection patients to ampicillin is up to 48.1%, highlighting a significant and escalating issue of AMR. In response to the growing threat of AMR, researchers have turned their attention to nitrogen-rich organic linkers, particularly diazoamino compounds, as a promising avenue for drug discovery.

Featuring a linear arrangement of three nitrogen atoms (N=N-NH), diazoamino, also known as triazene, belongs to a subgroup of azo compound and is considered one of the most favourable organic linkers due to its straightforward synthesis method, ease of availability [4], and cost-effectiveness [5]. Diazoamino has demonstrated potential in various

fields, such as photovoltaic applications [6], serving as a versatile linker in the systemisation of bioconjugates [7], heterocycles compound formations [8] as well as solid-phase synthesis [9]. It is noteworthy that the initial discovery of diazoamino was made by Griess and Hofmann (1859) during their research on the synthesis of 1,3-bis(phenyl) triazene, which is well-known for its symmetrical structural arrangement. Since then, research on diazoamino has escalated, particularly following its recognition for biological applications, including its roles as antibacterial [11], anti-inflammatory [12], and antiproliferative [7] agents. Moreover, dacarbazine (DTIC), a chemotherapy drug containing a diazoamino moiety in its structure, continues to be utilised in clinical medicine [13]. Additionally, to combat trypanosomiasis, veterinary medicine uses trypanocidal medications, such as isometamidium chloride (Samorin) and diminazene aceturate (Berenil), both of which incorporate diazoamino moieties [14].

Consequently, this study was initiated to synthesise a diazoamino linker through the diazo-coupling reaction of *p*-anisidine with halogenated aniline derivatives for further *in vitro* assessment of its biological efficiency against *E. coli* and *S. aureus* bacteria. The *p*-anisidine, which contains a methoxy group, was selected as the main component in the synthesis due to its known activation capabilities [15] by donating electrons and induces distortion in the aromatic ring system, resulting in intramolecular charge transfer that enhances selectivity and contributes to the antimicrobial activity of the compound [16,17]. Furthermore, methoxy has the ability to serve as a nucleophilic functional groups due to the presence of a lone pair of electrons, enabling it to form a covalent bond with a biological target [67]. On the other hand, halogen substituents, which are electron-withdrawing groups, were introduced due to their electronegativity properties which significantly increase the biological potential of a molecule [18] as reported in precedent literature. Moreover, it is anticipated that the presence of a halogen group may enhance the interaction of the compound with the bacterial receptor through halogen bonding [19], which can suscept the enzyme receptor [20] and increase binding affinity [21]. Both of these factors are crucial for bacterial inhibition. *In silico* molecular docking studies were performed to gain a better understanding of the ligand-receptor interactions that contribute to this activity. Additionally, a comprehensive evaluation of their drug-likeness and bioavailability was conducted using online tools to assess absorption, distribution, metabolism, excretion, and toxicity (ADMET) parameters. This research significantly enhances an understanding of the interactions between the synthesised compounds and

the targeted bacteria, while also indirectly contributing to the search for alternative potential drugs to address the issue of AMR.

Materials and Methods

Materials

All commercially available chemicals, including reagents (Merck KGaA) and solvents used in the experiment, were used without purification. The infrared spectra were obtained using the attenuated total reflectance (ATR) technique with a Perkin-Elmer Spectra GX Fourier transform infrared (FTIR) spectrometer, whilst the carbon, hydrogen, and nitrogen (CHN) elemental analyses were performed using a Thermo-FLASH EA 1112 series instrument. For ¹H and ¹³C nuclear magnetic (NMR) spectra, the data were recorded using a JEOL ECA 500 spectrophotometer at 500 MHz (¹H NMR) and 125 MHz (¹³C NMR) with acetone-d₆ as the standard reference expressed in δ ppm. Melting points were determined using a Stuart SMP10 instrument utilising a one-end closed capillary tube.

Synthesis of halogenated 4-methoxyphenyl-triazene (1-9)

The starting material, *p*-anisidine (3 mmol) was dissolved in ethanol and diazotised with 3M hydrochloric acid (HCl) and sodium nitrite (NaNO₂) (3 mmol) at 0-5 °C for 15 min. Upon observing a colour change, indicated by the potassium iodide (KI) starch paper, the pH was adjusted to a range of 5-6 with 5% sodium acetate (NaOAc). Subsequently, a coupling reagent, consisting of halogenated aniline derivatives (3 mmol), was introduced into the solution. The mixture was continuously stirred for approximately 45 min during which the reaction progress was monitored via thin-layer chromatography (TLC). The resulting crude product was filtered, washed with cold distilled water, and then dried at room temperature. Recrystallisation was performed using hot absolute ethanol.

Kirby-Bauer disk diffusion

The preliminary screening was conducted using the Kirby-Bauer disk diffusion method by employing two bacterial strains: *Escherichia coli* ATCC 25922 and *Staphylococcus aureus* ATCC 25923. The preparation began by culturing the bacteria in Luria-Bertani (LB) broth (10 mL), which was then incubated overnight at 37 °C with shaking at 200 rpm. Mueller-Hinton (MH) agar powder was used to prepare the agar plates. After sterilisation, 20 mL of the agar was poured into a plate. The bacteria turbidity followed the MacFarland standard, $0.5 \leq x \leq 0.51$ abs. Inoculation was performed using the streaking technique, where sterilised filter paper (6 mm) infused with 12 ppm of the test compounds and controls were placed on the agar surface. The triplicate of agar plates was

measured using a ruler (mm) following incubation for 24 h at 37 °C.

Turbidimetric kinetic assay

Turbidimetry assay was employed to determine the minimum inhibitory concentration (MIC) of selected compounds. For this assay, ampicillin was used as the positive control, while dimethyl sulfoxide (DMSO) served as the negative control. The bacteria were grown in a manner consistent with the preliminary test. Meanwhile, the positive control and compounds were prepared at dilutions of 50, 80, and 100 ppm. A vial containing bacteria (100 ppm) and broth (10 mL) was then supplemented with the compounds prepared at the specified dilutions, followed by incubation at 37 °C with shaking at 180 rpm. The data were collected at hourly intervals over a 6 h period using a UV-visible spectrophotometer at the transmittance (T) of 560 nm wavelength. The T value corresponds to the $\ln N_t$ in the graph which is translated to the number of colony forming units (CFU) per mL. Calculations were performed using the equations $\ln N_t = 27.4 - 10.3T$ for *S. aureus* and $\ln N_t = 27.1 - 8.56T$ for *E. coli*, as referenced in previous studies [22, 23].

Molecular docking

The crystal structures of meso-diaminopimelate ligase (MurE) (PDB ID:7B6M) and carotenoid dehydrosqualene synthase (CrtM) (PDB ID:3ACX) were retrieved from the RCSB protein data bank. The proteins were prepared using the Protein Preparation Wizard of Schrödinger's Maestro 2023-3 (version: 13.7.125) whereby for 7B6M, the chain A, unneeded water molecules, and the EDO ligand were removed whereas for 3ACX only water molecules were removed [24]. The binding sites were defined by selecting the protein's cocrystal structures N-[2-(2,5-Dioxopyrrolidin-1-yl)ethyl]-3-methylbenzamide (SZN) in 7B6M and N-(1-methylethyl)-3-[(3-prop-2-en-1-ylbiphenyl-4-yl)oxy]propan-1-amine (BPH673) in 3ACX with the Schrodinger Receptor Grid Generation module. The novel-designed ligands **1** (H), **2** (*o*-F), **4** (*p*-F) and **5** (*o*-Cl) were prepared using the LigPrep module of the Schrödinger suite with default settings. The prepared ligands were docked into the cocrystal binding site of proteins using the Glide module of Schrodinger in SP (Standard Precision) mode [25]. The glide scores were compared with those of the cocrystal and ampicillin, which served as standard drugs. The docking results were visualized using Discovery Studio 2024 Visualizer to

obtain the 2D interaction diagram and overlays of the docking results.

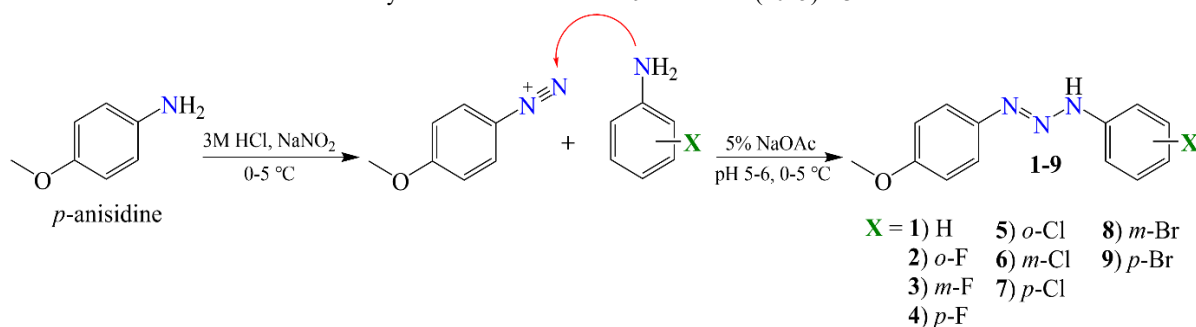
Pharmacokinetic evaluation

The investigation of drug bioavailability and likeliness investigation was conducted using readily available online tools which are pkCSM [<https://biosig.lab.uq.edu.au/pkcsm/prediction>]. The well-known pkCSM website was selected for its accessible and diverse ADMET parameters in antibacterial drug discovery [26]. The structures of compounds **1-9** including the controls (Ampicillin and Dacarbazine) were generated using ChemDraw 20.1 and formatted in SMILES notations. These structures were then utilised in the aforementioned tools to obtain the prediction results.

Results and Discussion

Chemical structural elucidation

Preceding compounds **1-9** were synthesised through the diazotisation of *p*-anisidine based on specified reaction conditions [27], followed by coupling with halogenated aniline at different positions as depicted in **Scheme 1**. During the coupling processes, challenges arose with coupling reagents at *ortho*- and *meta*-positions which failed to yield the desired products when 5% NaOH was used as a base for pH adjustment. It is important to note that the choice of base during the coupling process is crucial for the efficiency of triazene formation, as it serves to deprotonate the amine and enhance its reactivity towards the diazonium ions generated in the diazotisation stage. To address this issue, 5% NaOAc was introduced to successfully adjust the pH of the mixture to 5-6, resulting in the targeted triazene **1-9**. The use of NaOAc in the coupling reaction helps maintain a milder basic pH [28] while preventing the decomposition of aniline derivatives [29,30]. However, the reaction involving the *ortho*-bromoaniline coupling reagent, which was expected to yield (*E*)-3-(2-bromophenyl)-1-(4-methoxyphenyl) triaz-1-ene, was unsuccessful due to the weak *ortho*-directing ability of bromine, which adversely affected the regioselectivity of the reaction [31], in addition to high steric hindrance and relatively low basicity [66]. All other compounds were obtained in low to moderate yields (13-56%), likely due to the low solubility of the starting material, *p*-anisidine [32]. In this context, the use of polar solvents (ethanol, methanol, acetone) may not be optimal for efficiently dissolving *p*-anisidine, given its non-polar characteristics [33].



Scheme 1. Reaction pathway of compound 1-9

Following the completion of the synthesis of halogenated triazene derivatives, compounds 1-9 underwent structural confirmation *via* FTIR, ^1H , and ^{13}C NMR spectroscopies. Compound 3 was further analysed in detail for its characterisation, while the data for the other compounds are presented in the **Supplementary Materials**. In the FTIR spectral analysis, the presence of a methoxy substituent resulted in the appearance of peaks corresponding to $\nu_{(\text{CH}_3)}$ at 3022 cm^{-1} and $\nu_{(\text{C-O})}$ at around $1034\text{-}1196 \text{ cm}^{-1}$ [34]. Additionally, a strong absorption band observed at 1464 cm^{-1} corresponded to $\nu_{(\text{N=N})}$, while the adsorption band at 3183 cm^{-1} , assigned to the $\nu_{(\text{NH})}$ confirmed the formation of diazoamino ($-\text{N}=\text{N}-\text{NH}$) [11]. In the ^1H NMR characterisation, a singlet peak at δ_{H} 11.58 ppm could be attributed to the NH proton of the triazene moiety. The deshielded nature of this peak is due to the inherent deshielding effect associated with the NH group [35], which may be further amplified by hydrogen bonding interactions [36]. Moreover, the presence of a methoxy group ($-\text{OCH}_3$) was confirmed by a singlet peak at approximately δ_{H} 3.83 ppm. The chemical shift value for this peak aligns well with the expected range for methoxy resonances [37]. The aromatic protons were detected within the range of δ_{H} 6.94 to 7.45 ppm. Meanwhile, in the ^{13}C NMR spectroscopy, aromatic carbon signals appeared in the range of δ_{C} 105.3 to 131.8 ppm. The presence of the OCH_3 was evident from a singlet peak in the upfield region observed at δ_{C} 55.9 ppm [38], which could be attributed to electron-donating characteristics of methoxy [39]. Additionally, the resonance in the higher field region at δ_{C} 163.5 ppm is attributed to the C-O bond attached to the benzene ring. The peak at δ_{C} 165.4 ppm corresponds to the C-F attachment, with the higher value indicating the fluorine attachment due to its higher electronegativity compared to the OCH_3 [40].

Preliminary antibacterial screening

The Kirby-Bauer disk diffusion method was employed to evaluate the synthesised halogenated 4-methoxyphenyl-triazene derivatives, 1-9 as a preliminary screening against both Gram-negative (*E. coli*) and Gram-positive (*S. aureus*) bacteria and the

data obtained are tabulated in **Table 1**. This preliminary screening aimed to facilitate the selection process and assess the initial biological activity of compounds that require further investigation. Overall, the data indicated that most of the compounds exhibited greater inhibition against the *S. aureus* strain compared to the *E. coli* strain. Although *S. aureus* possesses a thicker peptidoglycan cell wall, it lacks the protective outer layer membrane [41], making it more susceptible to the tested compounds rather than against the *E. coli* strain. In contrast to the other compounds, compound 9 (*p*-Br) demonstrated no antibacterial effect against either strain. This lack of activity may be attributed to the lower electronegativity of bromine [42], as evidenced by the results of compounds 8 and 9, which show minimal to no inhibition against both strains. By comparing the overall trend between the positional differences against both strains, the inhibition zones followed the order of *ortho*, *para* > *meta*, with compounds 4 (*p*-F) and 5 (*o*-Cl) exhibiting the strongest inhibition against *S. aureus* ($10.0 \pm 0.00 \text{ mm}$) and *E. coli* (compound 5 (*o*-Cl), $8.9 \pm 0.25 \text{ mm}$). The promising inhibitory effect of compound 5 (*o*-Cl) against both tested strains may be attributed to the synergistic interaction between the parent structure (*p*-anisidine) and the halogen substituent at a specific location (*ortho*-positioned) [21]. This interaction can enhance the binding affinity of the compound, thereby effectively inhibiting bacterial growth [43]. Meanwhile, compound 4 which contains a *para*-fluoro substituent was found to be more effective against *S. aureus* rather than *E. coli*. This selective substitution of fluorine at the less sterically-hindered *para* position eventually strengthened the carbon fluoro bond [44] leading to effective inhibition [45].

Antibacterial activity

Following the selection of compounds with the most prominent inhibition zones of $\geq 8.8 \text{ mm}$ in the disk diffusion assay of compounds 1-9, further minimum inhibitory concentration (MIC) determination was performed on compounds 1 (H), 2 (*o*-F), 4 (*p*-F), and 5 (*o*-Cl) *via* turbidimetric kinetic assay against the same strains, *E. coli* and *S. aureus*. The results of the

turbidimetric assay for the selected compounds are illustrated in a graph of $\ln N_t$ against time (h), as depicted in **Supplementary Materials** for both strains. All selected compounds demonstrated MIC results of less than 200 ppm which aligns with the criteria established [46] for potential medical applications. The minimum concentration required to inhibit the growth of *S. aureus* and *E. coli*, $\mu = 0$ [47,48] was extrapolated in the graph depicted in **Figure 1 (a)** *S. aureus* and **(b)** *E. coli* for compounds **1**, **2**, **4**, and **5**.

From the results presented in **Table 2**, it is evident that compound **1** (H) exhibited the lowest MIC against the *S. aureus* strain, with MIC value of 87 ppm, outperforming the standard drug ampicillin, which has MIC value of 96 ppm. The lower molecular weight of compound **1** enhances its efficacy as a bioactive component, allowing it to penetrate and reach the target sites within the bacteria [11]. Conversely, the assessment of the compounds against *E. coli* revealed that the replacement of H in **1** with *ortho*-chloro as in **5** demonstrated potent antibacterial activity with the MIC of 82 ppm outperforming the standard drug ampicillin (127 ppm). This could be due to the lipophilic characteristics of the chlorine atom that is well suited to the lipophilic amino acid residues of the bacteria strains [49]. Not only that, the addition of a halogen bond in the compound is able to escalate the interaction of protein-ligand binding [50] owing to the

presence of halogen bond donor sites [51] with the phosphate or oxygen acceptor in the phospholipid bilayer [21].

Interestingly, the MIC against *E. coli* results suggest that compounds **4** (*p*-F), and **5** (*o*-Cl) gave a lower MIC value of 89 and 82 ppm, respectively compared to *S. aureus* strains regardless of their potent inhibition in the disk diffusion results. The observed difference in the MIC could be partially attributed to the enzymatic degradation by the gram-positive *S. aureus*, weakening the compound's binding abilities between the target sites. Overall, the MIC trend for the tested compounds **1** (H) and **2** (*o*-F) appears to be aligned with the preliminary disk diffusion results suggesting a higher susceptibility of *S. aureus* compared to *E. coli*.

Molecular docking analysis

Subsequent to the *in vitro* evaluation with promising minimum inhibitory concentration (MIC) showed by compounds **1** (H), **2** (*o*-F), **4** (*p*-F) and **5** (*o*-Cl), further molecular docking analysis was performed to outline the interactions between compounds acting as a ligand and the proteins serving as a biological receptor that responsible for the activity [52]. The docking was conducted by using Schrödinger Maestro version 13.7.125 software targeting meso-diaminopimelate ligase (MurE) (PDB ID: 7B6M) for *E. coli* and dehydrosqualene synthase (CrtM) (PDB ID: 3ACX)

Table 1. Inhibition zone (mm) results

Compound	Inhibition zone (mm)	
	<i>E. coli</i>	<i>S. aureus</i>
1 (H)	8.1 ± 0.25	9.0 ± 0.00
2 (<i>o</i> -F)	7.9 ± 0.25	8.8 ± 0.29
3 (<i>m</i> -F)	-	8.3 ± 0.50
4 (<i>p</i> -F)	7.1 ± 0.25	10.00 ± 0.00
5 (<i>o</i> -Cl)	8.9 ± 0.25	10.00 ± 0.00
6 (<i>m</i> -Cl)	-	8.5 ± 0.00
7 (<i>p</i> -Cl)	-	6.6 ± 0.25
8 (<i>m</i> -Br)	-	8.1 ± 0.25
9 (<i>p</i> -Br)	-	-
Ampicillin	11.1 ± 0.25	13.0 ± 0.65

Note: (-) no inhibition

Table 2. Minimum Inhibitory Concentration (ppm) results

Compound	Minimum Inhibitory Concentration (MIC)	
	<i>E. coli</i>	<i>S. aureus</i>
1 (H)	121	87
2 (<i>o</i> -F)	117	94
4 (<i>p</i> -F)	89	101
5 (<i>o</i> -Cl)	82	94
Ampicillin	127	96

for *S. aureus* comparing to the standard ampicillin. The MurE enzyme which belongs to the Mur ligase family was chosen due to its importance for cell wall synthesis, particularly the peptidoglycan [53] whereas CrtM was for its importance in staphyloxanthin production in MRSA bacterium [54]. Disruption of these enzymes will stop cell proliferation and cause cell death. The binding sites were defined through the

Schrödinger Receptor Grid Generation module by selecting SZN and BPH673 co-crystals in MurE and CrtM protein respectively. This step is important for parameter validation [55] and ensures that the docking of the synthesised ligand takes place within the designated binding pockets as illustrated in **Figures 2 and 3**.

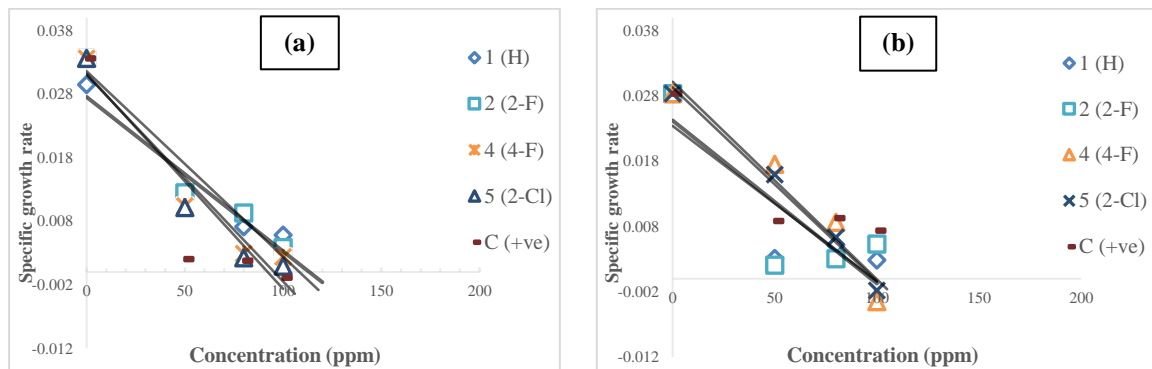


Figure 1. The MIC of compounds 1, 2, 4, and 5 against (a) *S. aureus* and (b) *E. coli*

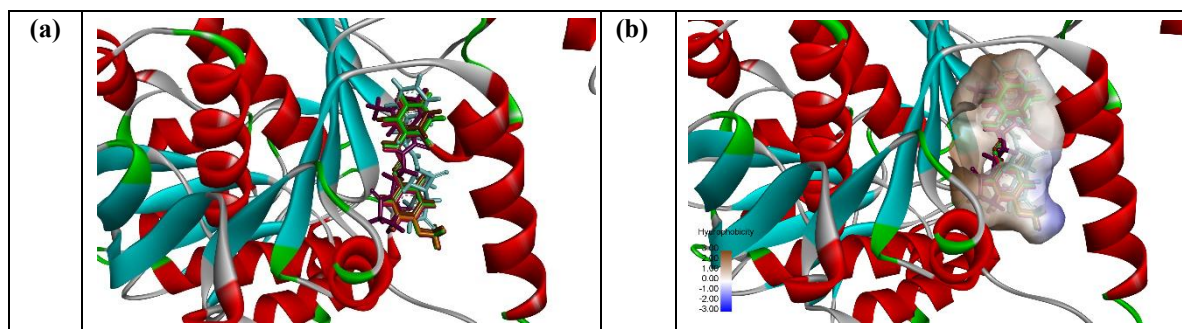


Figure 2. (a) Compounds 1 (H) (green), 2 (o-F) (orange), 4 (p-F) (pink), 7 (o-Cl) (brown), Cocrystral SZN (purple) and ampicillin (light blue) in the binding site of MurE and (b) Compounds 1 (H) (green), 2 (o-F) (orange), 4 (p-F) (pink), 7 (o-Cl) (brown), Cocrystral SZN (purple) and ampicillin (light blue) in the hydrophobic pocket of MurE.

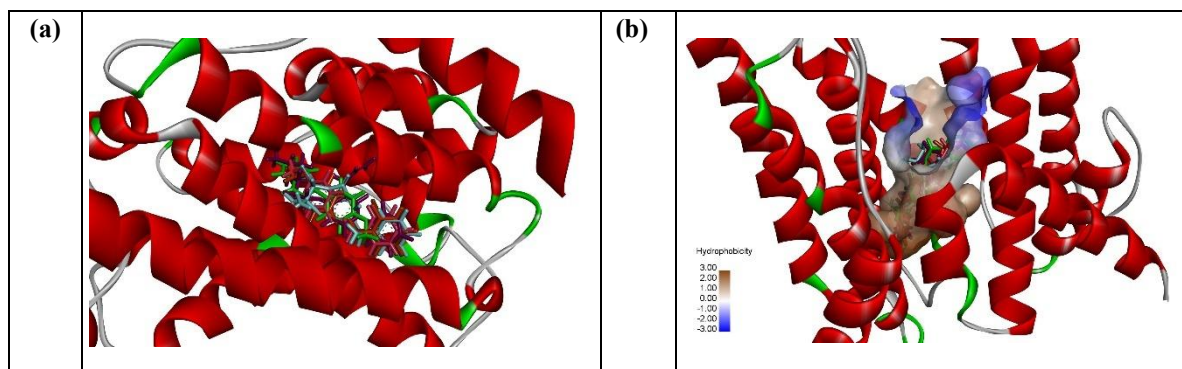


Figure 3. (a) Compounds 1 (H) (green), 2 (o-F) (orange), 4 (p-F) (pink), 7 (o-Cl) (brown), Cocrystral SZN (purple) and ampicillin (light blue) in the binding site of MurE and (b) Compounds 1 (H) (green), 2 (o-F) (orange), 4 (p-F) (pink), 7 (o-Cl) (brown), Cocrystral BPH673 (purple) and ampicillin (light blue) in the hydrophobic pocket of CrtM.

In the docking towards the MurE enzyme, compounds **1** (H), **2** (*o*-F), **4** (*p*-F), and **5** (*o*-Cl), demonstrated binding affinities ranging from -7.37 to -7.94 kcal/mol which are better than that of ampicillin (-6.92 kcal/mol). It can be observed in **Figure 4** that the major contribution to the higher binding energies of these compounds than ampicillin is the hydrogen bonding between the -NH group of the triazene linkage and the HOH779 water molecules which a similar interaction was also poised by the SZN cocrystal but not ampicillin. It is worth highlighting, compounds **2** (*o*-F) and **4** (*p*-F) which are among the highest binding energies have an extra hydrogen bonding formed between the fluorine atoms with TYR229 and HIS232 residues respectively. The presence of hydrogen bonding significantly contributes to the drug's solubility and permeability in biological targets [22, 56]. Therefore, the absence of the hydrogen bonding interaction in ampicillin might be the reason for better MIC exhibited by the synthesised compound in the *in vitro* study against *E. coli*. Apart from hydrogen bonds, the synthesised ligands also exhibited several other interactions such as *van der Waals* forces, π - π stacking, and π -alkyl interaction with the residues in proximity namely CYS234, GLY113, GLY246, ILE239, LEU189, PHE199, SER202, THR115, VAL184 and VAL194 similar to SZN, which contribute to the inhibition of the cell growth.

Likewise, similar trends were also portrayed in the dockings towards the CrtM protein where ampicillin (-7.23 kcal/mol) exhibited lower binding scores than ligands **1** (H), **2** (*o*-F), **4** (*p*-F), and **5** (*o*-Cl) which had scores ranging from -7.48 to -8.27 kcal/mol. Contrary to the previous, ampicillin and all tested compounds (*except compound 1 with only one H-bond*) exhibited a minimum of three hydrogen bonds with the amino acids residue in the CrtM binding pocket (**Figure 5**). Interestingly, compound **2** (*o*-F) which had the highest binding score of -8.27 kcal/mol, possessed a total of four hydrogen bonds formed from the -NH and the N=N of triazene linkage with ALA157 and GLY161

respectively as well as the -H of the methoxy with water molecules of HOH306 and HOH623. These hydrogen bond interactions with the receptors attest to the compounds' superiority in inhibiting bacterial growth [57]. Furthermore, the electrostatic interactions between the compounds and the key residues such in cocrystal BPH673, for instance, ALA134, CYS44, GLY138, HIS18, ILE241, LEU141, LEU145, LEU160, LEU164, PHE22, PHE233, PHE26, TYR41, VAL133, and VAL137 through *van der Waals* forces and π -alkyl interactions further anchored and stabilised the binding [58] disrupting cell integrity. The binding scores of the compounds towards MurE and CrtM proteins are tabulated in **Table 3**.

Pharmacokinetics information

Additional *in silico* studies for all synthesised 4-methoxyphenyl-triazene derivatives, **1-9**, were conducted targeting their drug-likeness and bioavailability which are crucial in the preliminary candidacy for prospective drugs [22]. In this case, Lipinski's Rule of Five (RO5) was utilised to evaluate the physicochemical properties of the compounds, which are commonly found in clinical drugs [59]. The controls in this analysis included ampicillin a widely used clinical drug [60] and dacarbazine, which were chosen for their structural similarities which feature important moieties such as N=N-NH [13] alongside with the synthesised compounds (**1-9**). Upon evaluating their properties, it was observed that all compounds obeyed Lipinski's RO5 with 0 violations as shown in **Table 4**. The RO5 analysis consists of 5 different parameters including molecular weight (MW) less than 500 g mol⁻¹ [61], rotatable bonds (≤ 10), hydrogen bond donor (≤ 5), and acceptor (≤ 10) all of which adhered by compounds **1-9** including the controls [62]. Moreover, all compounds also complied with the lipophilicity constant (less than 5) as well as topological polar surface area (TPSA) which is less than 130 Å [63].

Table 3. Binding affinity scores for compounds **1**, **2**, **4** and **5**

Compound	Binding affinity (Kcal/mol)	
	<i>E. coli</i> (<i>MurE</i>)	<i>S. aureus</i> (<i>CrtM</i>)
1 (H)	-7.37	-7.48
2 (<i>o</i> -F)	-7.76	-8.27
4 (<i>p</i> -F)	-7.94	-7.96
5 (<i>o</i> -Cl)	-7.26	-8.18
Ampicillin	-6.92	-7.23
Cocrystal	-8.00	-10.0

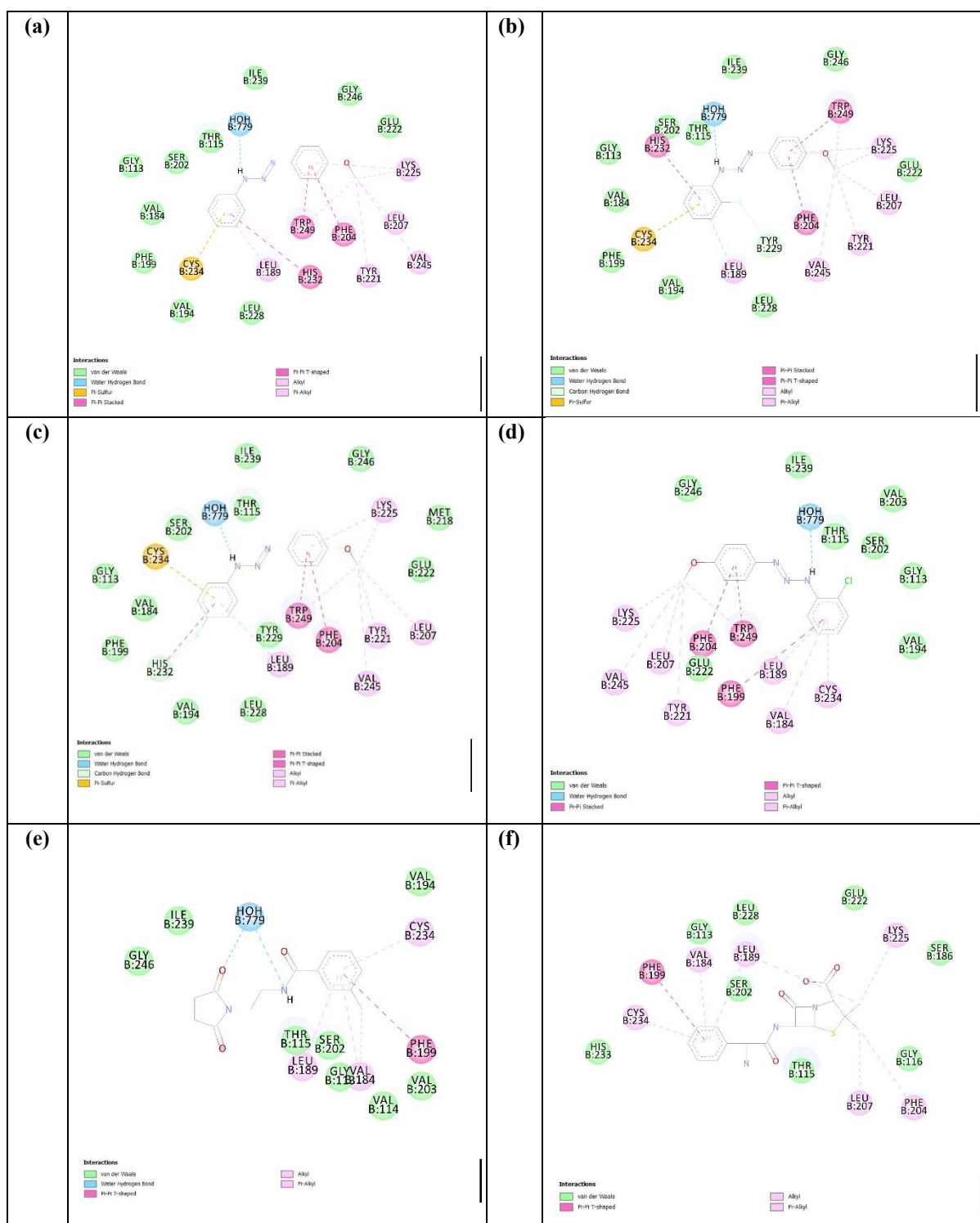


Figure 4. 2D interaction visualized by Discovery Studio 2024 (a) Compounds 1 (H) (b) 2 (*o*-F), (c) 4 (*p*-F) (d) 5 (*o*-Cl), (e) Cocystal SZN and (f) ampicillin in MurE protein binding site

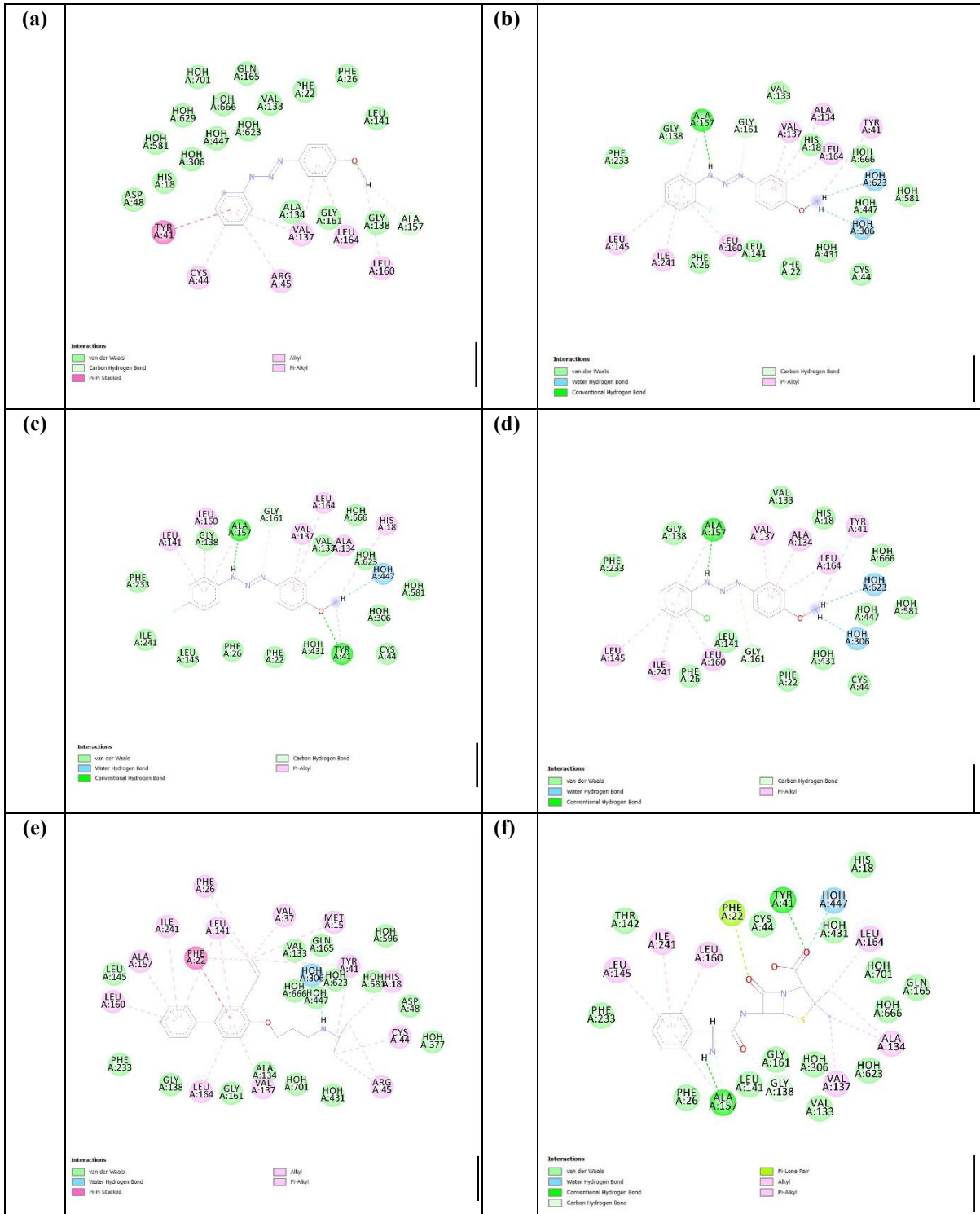


Figure 5. 2D interaction visualized by Discovery Studio 2024 (a) Compounds 1 (H) (b) 2 (*o*-F), (c) 4 (*p*-F) (d) 5 (*o*-Cl), (e) Cocystal BPH673 and (f) ampicillin in CrtM protein binding site

Table 4. The Lipinski's Rule of Five for compounds **1-9** and two positive controls

Compounds (Molecular Formula)	MW g mol ⁻¹	Rotatable Bonds	H-Bond (Donor)	H-Bond (Acceptor)	log <i>P</i> o/w	TPSA Å
1 (H)	227.3	4	1	3	3.8	99.9
2 (<i>o</i> -F)	245.1	4	1	4	3.4	104.1
3 (<i>m</i> -F)	245.1	4	1	3	3.9	104.1
4 (<i>p</i> -F)	245.1	4	1	4	3.6	104.1
5 (<i>o</i> -Cl)	261.1	4	1	4	3.9	110.2
6 (<i>m</i> -Cl)	261.7	4	1	3	4.5	110.2
7 (<i>p</i> -Cl)	261.7	4	1	3	4.5	110.2
8 (<i>m</i> -Br)	306.2	4	1	3	4.6	113.8
9 (<i>p</i> -Br)	306.2	4	1	3	4.6	113.8
Ampicillin	349.4	4	3	5	0.3	143.1
Dacarbazine	182.2	3	2	4	0.1	74.6

Note: MW = molecular weight; H-Bond = hydrogen bond; log *P* o/w = octanol/water partition coefficient; TPSA = topology polar surface area.

Table 5. ADMET profiling results for compounds **1-9** and two positive controls

Properties	1	2	3	4	5	6	7	8	9	Ampicillin	Dacarbazine
Absorption											
• Caco-2 permeability	High	Low	Low								
• HIA	Excellent	Moderate	Moderate								
• Skin Permeability	Low	Low									
Distribution											
• BBB Permeability	0.230	0.059	0.165	0.160	0.204	0.172	0.167	0.171	0.165	-1.262	-1.169
• CNS permeability	Excellent	Poor	Poor								
Metabolism (Inhibitor)											
• CYP1A2	Yes	No	No								
• CYP2C19	Yes	No	No								
• CYP2C9	No	Yes	No	No							
• CYP2D6	No	Yes	Yes	No	No						
• CYP3A4	No	No									
Excretion											
Total Clearance	-0.020	-0.130	-0.125	-0.122	0.278	0.148	0.086	0.126	0.064	0.263	0.163
Toxicity											
• AMES	Yes	Yes	No	Yes							
• Hepatotoxicity	No	Yes	Yes								
• hERG I & II Inhibitor	No	No									

Compounds **1-9** were further entailed on their ADMET (absorption, distribution, metabolism, excretion, and toxicity) properties *via* pkCSM tools, which employs a graph-based algorithm [64]. Based on the pharmacokinetic results in **Table 5**, in absorption parameters, the Caco-2 permeability properties of all compounds demonstrated high permeability compared to the control. Apart from that, all compounds exhibited excellent human intestinal absorption (HIA) of over 30% and a low skin permeability constant [61]. In terms of distribution parameter, all compounds showed a positive blood-brain barrier (log BBB < -1 and > 0.3) and an excellent central nervous system (CNS) (log PS > -2) absorption rate. Understanding these permeability properties is important for comprehending how a drug distributes into various organs and tissues [56]. The metabolism

parameter specifically targeted five different CYP P450 cytochromes that are crucial for enzyme detoxification in the human body [64]. While all compounds were inhibitors for CYP1A2, CYP2C1, and CYP2C9 (*except compound 1*), compounds **1-7** were identified as non-inhibitors of CYP2D6, and all compounds were non-inhibitors of CYP3A4. Regarding the excretion parameter, the total clearance for compounds **1-9** ranged from -0.020 to 0.278 log min⁻¹ kg⁻¹. Meanwhile for toxicity parameters that include AMES, hepatotoxicity, and hERG I and II inhibitors, all compounds, except for compounds **1** (H) and **2** (*o*-F), revealed to have no toxicity against the tested properties. The results of the *in silico* analysis suggest that the synthesised 4-methoxyphenyl-triazene derivatives could be considered as alternative compounds in drug design

[65].

Conclusion

A total of nine 4-methoxyphenyl-triazene derivatives were successfully synthesised through N-N diazo-coupling and characterised using elemental CHN analysis, FTIR, ¹H, and ¹³C NMR spectroscopies. The *in vitro* analyses conducted via turbidimetric kinetic assays revealed that compound **1** (H), which has the smallest atomic weight, was the most effective against *S. aureus* (87 ppm), while compound **5** (o-Cl) exhibited the highest efficacy against *E. coli* (82 ppm). Supported by molecular docking analyses targeting CrtM and MurE proteins, hydrogen bonding was identified as a key interaction contributing to the good binding affinity of the compounds. Furthermore, pharmacokinetic profiling indicated that all compounds adhered to the Lipinski's rule with zero violation, making them suitable candidates for oral drug development. In terms of ADMET profiling, nearly all compounds met the necessary reference points for the evaluated parameters. Nevertheless, compound **5**, with its *ortho*-chloro substituent, demonstrated the most optimal outcomes based on both *in vitro* and *in silico* analysis results. The attachment of both electron-donating (-OCH₃) and -withdrawing (Cl) groups in the respective phenyl rings, which coexist through the triazene (N=N-NH) linker, may elevate the maximum interaction between the compounds and the targeted bacteria. This suggests that this compound has the potential as an effective antibacterial agent.

Acknowledgement

The authors would like to give thanks to Universiti Malaysia Sarawak (UNIMAS) especially the Faculty of Resource Science and Technology (FRST) and Ministry of Higher Education, Malaysia for the assistance in research facilities and financial support through the FRGS funds (FRGS/1/2021/STG01/UNIMAS/03/2).

References

- Noriega, S., Cardoso-Ortiz, J., López-Luna, A., Cuevas-Flores, M. D. R., and Flores De La Torre, J. A. (2022). The diverse biological activity of recently synthesized nitro compounds. *Pharmaceuticals*, 15(6): 717.
- Kerru, N., Gummidi, L., Maddila, S., Gangu, K. K., and Jonnalagadda, S. B. (2021). A review on recent advances in nitrogen-containing molecules and their biological applications. *Molecules*, 25(8): 1909.
- Khwaza, V., Mlala, S., Oyedeji, O. O., and Aderibigbe, B. A. (2021). Pentacyclic triterpenoids with nitrogen-containing heterocyclic moiety, privileged hybrids in anticancer drug discovery. *Molecules*, 26(9): 2401.
- Tahir, T., Shahzad, M. I., Tabassum, R., Rafiq, M., Ashfaq, M., Hassan, M., Kotwica-Mojzych, K., and Mojzych, M. (2021). Diaryl azo derivatives as anti-diabetic and antimicrobial agents: Synthesis, *in vitro*, kinetic and docking studies. *Journal of Enzyme Inhibition and Medicinal Chemistry*, 36(1): 1509-1520.
- Li, L., Xu, F., Sun, G., Sun, M., Jia, S., Li, H., Xu, T., Zhang, H., Wang, Y., Guo, Y., and Liu, T. (2021). Identification of N-methylaniline based on azo coupling reaction by combining TLC with SERRS. *Spectrochimica Acta - Part A: Molecular and Biomolecular Spectroscopy*, 252: 119490.
- Saeed, A., Nasher, M. A., Abdel-Latif, E., Keshk, E. M., Khalil, A. G. M., and Metwally, H. M. (2019). New derivatives of azopyrazolo dyes: Synthesis and optical characterization for application in sensitized solar cells. *Optik*, 196: 163036.
- Davis, G. J., Townsend, J. A., Morrow, M. G., Hamie, M., Shepard, A. J., Hsieh, C. C., Marty, M. T., and Jewett, J. C. (2021). Protein modification via mild photochemical isomerization of triazenes to release aryl diazonium ions. *Bioconjugate Chemistry*, 32(11): 2432-2438.
- Tan, J. F., Bormann, C. T., Perrin, F. G., Chadwick, F. M., Severin, K., and Cramer, N. (2019). Divergent synthesis of densely substituted arenes and pyridines via cyclotrimerization reactions of alkynyl triazenes. *Journal of the American Chemical Society*, 141(26): 10372-10383.
- Wippert, N. A., Jung, N., and Bräse, S. (2019). Synthesis of arylamides via ritter-type cleavage of solid-supported aryltriazenes. *ACS Combinatorial Science*, 21(8): 568-572.
- Griess, P., and Hofmann. (1859). V. On new nitrogenous derivatives of the phenyl- and benzoyl-series. *Proceedings of the Royal Society of London*, 9: 594-597.
- Abd Halim, A. N., Mohammad Hussin, A. S., Ngaini, Z., Zamakshshari, N. H., and Haron, I. Z. (2023). Synthesis, antibacterial potential and *in silico* molecular docking analysis of triazene compounds via diazo coupling reactions of an amine. *Tetrahedron Letters*, 132: 154803.
- Jaiswal, S., and Verma, K. N. (2021). Benzothiazole moiety with sulphonamide as anti-inflammatory and analgesic activity: A review. *South Asian Research Journal of Pharmaceutical Sciences*, 3(6): 90-102.
- Rydén, V., El-Naggar, A. I., Koliadi, A., Ladjevardi, C. O., Digkas, E., Valachis, A., and Ullenhag, G. J. (2024). The role of dacarbazine

- and temozolomide therapy after treatment with immune checkpoint inhibitors in malignant melanoma patients: A case series and meta-analysis. *Pigment Cell and Melanoma Research*, 37(3): 352-362.
14. Eghianruwa, K. I., and Oridupa, O. A. (2018). Chemotherapeutic control of trypanosomiasis - A review of past measures, current status and future trends. *Veterinarski Arhiv*, 88(2): 245-270.
 15. Solomons, G., Fryhle, C., and Snyder, S. (2014). *Organic Chemistry* (11th edition). John Wiley & Sons, Hoboken: pp. 509.
 16. Pathak, S., Kumar, A., and Tandon, P. (2010). Molecular structure and vibrational spectroscopic investigation of 4-chloro-4'-dimethylamino-benzylidene aniline using density functional theory. *Journal of Molecular Structure*, 981: 1-9.
 17. Govindarasu, K., and Kavitha, E. (2014). Vibrational spectra, molecular structure, NBO, UV, NMR, first order hyperpolarizability, analysis of 4-Methoxy-4'-Nitrobiphenyl by density functional theory. *Spectrochimica Acta - Part A: Molecular and Biomolecular Spectroscopy*, 122: 130-141.
 18. Jain, S., Dayma, V., Sharma, P., Bhargava, A., Baroliya, P. K., and Goswami, A. K. (2019). Synthesis of some new hydroxytriazenes and their antimicrobial and anti-inflammatory activities. *Anti-Inflammatory & Anti-Allergy Agents in Medicinal Chemistry*, 19(1): 50-60.
 19. Ngaini, Z., and Mortadza, N. A. (2019). Synthesis of halogenated azo-aspirin analogues from natural product derivatives as the potential antibacterial agents. *Natural Product Research*, 33(24): 3507-3514.
 20. Naseem, H. A., Aziz, T., Shah, H. ur R., Ahmad, K., Parveen, S., and Ashfaq, M. (2021). Rational synthesis and characterization of medicinal phenyl diazenyl-3-hydroxy-1h-inden-1-one azo derivatives and their metal complexes. *Journal of Molecular Structure*, 1227: 129574.
 21. Faleye, O. S., Boya, B. R., Lee, J. H., Choi, I., and Lee, J. (2024). Halogenated antimicrobial agents to combat drug-resistant pathogens. *Pharmacological Reviews*, 76(1): 90-141.
 22. Abd Halim, A. N., Mohammad Hussin, A. S., Ngaini, Z., Sing, N. N., Jong, S. A., and Saberi, M. M. M. (2023). Synthesis, in vitro and in silico studies of alkylated paracetamol derivatives as potential antibacterial agent. *Borneo Journal of Resource Science and Technology*, 13(2): 161-174.
 23. Ngaini, Z., Rasin, F., Wan Zullkiplee, W. S. H., and Abd Halim, A. N. (2020). Synthesis and molecular design of mono aspirinate thiourea-azo hybrid molecules as potential antibacterial agents. *Phosphorus, Sulfur and Silicon and the Related Elements*, 196(3): 275-282.
 24. Rajagopal, K., Varakumar, P., Aparna, B., Byran, G., and Jupudi, S. (2021). Identification of some novel oxazine substituted 9-anilinoacridines as SARS-CoV-2 inhibitors for COVID-19 by molecular docking, free energy calculation and molecular dynamics studies. *Journal of Biomolecular Structure and Dynamics*, 39(15): 5551-5562.
 25. Wen, T., Wang, J., Lu, R., Tan, S., Li, P., Yao, X., Liu, H., Yi, Z., Li, L., Liu, S., Gao, P., Qian, H., Xie, G., and Ma, F. (2023). Development, validation, and evaluation of a deep learning model to screen cyclin-dependent kinase 2 inhibitors in cancers. *European Journal of Medicinal Chemistry*, 250(2): 115199.
 26. Ahmad, I., Kuznetsov, A. E., Pirzada, A. S., Alsharif, K. F., Daglia, M., and Khan, H. (2023). Computational pharmacology and computational chemistry of 4-hydroxyisoleucine: Physico chemical, pharmacokinetic, and DFT-based approaches. *Frontiers in Chemistry*, 11: 1145974.
 27. Abdel-Aty, A. S., Desheesh, M. A., Abdallah, E. S. A. M., Osama, D. A., and Amer, H. A. (2023). Antimicrobial effects of some diazoamino benzene derivatives. *Egyptian Journal of Chemistry*, 66(13): 137-144.
 28. Maghsoodlou, M. T., Safarzaei, M., Mousavi, M. R., Hazeri, N., Aboonajmi, J., and Shirzaei, M. (2014). A green and novel three-component one-pot synthesis of tetrahydrobenzopyran, pyrano [2, 3-d] pyrimidine, and 3, 4-dihydropyrano [c] chromene derivatives using sodium acetate. *Iran Journal of Organic Chemistry*, 6(1): 1197-1202.
 29. Melardi, M. R., Shamsi Mogoi, F. B., Sajirani, A. B., Gharamaleki, J. A., Notash, B., and Rofouei, M. K. (2015). Synthesis, characterization and crystal structure of four new asymmetric triazene ligands: An example of linear HgII complex with Hg. π secondary bonding interactions. *Journal of Chemical Sciences*, 127(12): 2171-2181.
 30. Aydin, H., Akocak, S., Lolak, N., Uslu, U., Sait, A., Korkmaz, S., Parmaksiz, A., Ceylan, O., and Aksakal, A. (2023). *In vitro* multitarget activity of sulfadiazine substituted triazenes as antimicrobial, cytotoxic, and larvicidal agents. *Journal of Biochemical and Molecular Toxicology*, 37(10): e23467.
 31. Luliński, S., and Serwatowski, J. (2003). Bromine as the ortho-directing group in the aromatic metalation/silylation of substituted bromo benzenes. *Journal of Organic Chemistry*, 68(24): 9384-9388.
 32. Baker, L. M., Aimon, A., Murray, J. B., Surgenor, A. E., Matassova, N., Roughley, S. D., Collins, P. M., Krojer, T., von Delft, F., and Hubbard, R. E. (2020). Rapid optimisation of fragments and hits to lead compounds from screening of crude

- reaction mixtures. *Communications Chemistry*, 3(1): 122.
33. Canal-Martín, A., Navo, C. D., Sáez, E., Molero, D., Jiménez-Osés, G., and Pérez-Fernández, R. (2021). Nucleophilic catalysis of: p-substituted aniline derivatives in acylhydrazone formation and exchange. *Organic and Biomolecular Chemistry*, 19(33): 7202-7210.
 34. Kantar, C., Baltas, N., Karaoğlu, Ş. A., and Şaşmaz, S. (2018). Some azo dyes containing eugenol and guaiacol, synthesis, antioxidant capacity, urease inhibitory properties and anti-helicobacter pylori activity. *Revue Roumaine de Chimie*, 63(3): 189-197.
 35. Landman, I. R., Suleymanov, A. A., Fadaei-Tirani, F., Scopelliti, R., Chadwick, F. M., and Severin, K. (2020). Brønsted and Lewis acid adducts of triazenes. *Dalton Transactions*, 49(7): 2317-2322.
 36. Feng, S. biao, Li, F. sheng, Zhao, X. yuan, Qian, Y. dong, Fei, T., Yin, P., and Pang, S. P. (2021). Comparative study on 1,2,3-triazole based azo- and triazene-bridged high-nitrogen energetic materials. *Energetic Materials Frontiers*, 2(2): 125-130.
 37. Nabatipour, S., Mohammadi, S., and Mohammadi, A. (2020). Synthesis and comparison of two chromone based Schiff bases containing methoxy and acetamido substitutes as highly sustainable corrosion inhibitors for steel in hydrochloric acid. *Journal of Molecular Structure*, 1217: 128367
 38. Ngaini, Z., Hissam, M. A., Mortadza, N. A., Abd Halim, A. N., and Daud, A. I. (2023). *In vitro* antimicrobial activities, molecular docking and density functional theory (DFT) evaluation of natural product-based vanillin derivatives featuring halogenated azo dyes. *Natural Product Research*, 1-11.
 39. Pavia, D. L., Lampman, G. M., Kriz, G. S., & Vyvyan, J. R. (2013). Introduction to Spectroscopy (5th edition). Cengage Learning, Stamford: pp. 619.
 40. Cheng, H. G., and Yin, G. (2019). Nucleophilic α -fluorination of Amides. *Chem*, 5(5), 1022-1024.
 41. Kmiecik, A., Krzeminski, P. M., Hodii, A., Gorczyca, D., and Jastrzebska, A. (2024). New water-soluble (iminomethyl)benzenesulfonates derived from biogenic amines for potential biological applications. *Materials*, 17: 520.
 42. Nilchan, N., Phetsang, W., Nowwarat, T., Chaturongakul, S., and Jiarpinitnun, C. (2018). Halogenated trimethoprim derivatives as multidrug-resistant Staphylococcus aureus therapeutics. *Bioorganic and Medicinal Chemistry*, 26(19): 5343-5348.
 43. Di Martino, M., Sessa, L., Di Matteo, M., Panunzi, B., Piotto, S., and Concilio, S. (2022). Azobenzene as antimicrobial molecules. *Molecules*, 27(17): 5643.
 44. Ghorab, M. M., Alsaid, M. S., El-Gaby, M. S. A., Elaasser, M. M., and Nissan, Y. M. (2017). Antimicrobial and anticancer activity of some novel fluorinated thiourea derivatives carrying sulfonamide moieties: Synthesis, biological evaluation and molecular docking. *Chemistry Central Journal*, 11(1): 32.
 45. Bilginer, S., Gonder, B., Gul, H. I., Kaya, R., Gulcin, I., Anil, B., and Supuran, C. T. (2020). Novel sulphonamides incorporating triazene moieties show powerful carbonic anhydrase I and II inhibitory properties. *Journal of Enzyme Inhibition and Medicinal Chemistry*, 35(1): 325-329.
 46. Chee, D. N. A., Rodis, M. L., Saat, N., Ngaini, Z., and Halim, A. N. A. (2017). Synthesis and antibacterial study of organotin(IV) complexes containing hydrazinopyridine ligand. *Malaysian Journal of Analytical Sciences*, 21(5): 1143-1150.
 47. De Los Angeles Alvarez, M., Zarelli, V. E. P., Pappano, N. B., and Debattista, N. B. (2004). Bacteriostatic action of synthetic polyhydroxylated chalcones against *Escherichia coli*. *Biocell*, 28(1): 31-34.
 48. Rani, A., and Jain, S. (2008). Studies on *Enterococcus faecium* growth-inhibitory action of 1, 5-BIS (2-hydroxyphenyl)pent-1, 4-diene-3-one and related compounds: A search for environmentally benign anti-bacterial agent. *Rasayan Journal of Chemistry*, 1(4): 795-801.
 49. Chiodi, D., and Ishihara, Y. (2023). "Magic Chloro": Profound effects of the chlorine atom in drug discovery. *Journal of Medicinal Chemistry*, 66(8): 5305-5331.
 50. Shinada, N. K., De Brevern, A. G., and Schmidtke, P. (2019). Halogens in protein-ligand binding mechanism: A structural perspective. *Journal of Medicinal Chemistry*, 62(21): 9341-9356.
 51. Govindaraj, V., Ungati, H., Jakka, S. R., Bose, S., and Mughesh, G. (2019). Directing traffic: Halogen bond-mediated membrane transport. *Chemistry - A European Journal*, 25(48): 11180-11192.
 52. Miladiyah, I., Jumina, J., Haryana, S. M., & Mustofa, M. (2018). Biological activity, quantitative structure-activity relationship analysis, and molecular docking of xanthone derivatives as anticancer drugs. *Drug Design, Development and Therapy*, 12: 149-158.
 53. Kumar, A., Singh, P., Singh, E., Jain, M., Muthukumar, J., and Singh, A. K. (2024). In silico strategies for identifying therapeutic

- candidates against *Acinetobacter baumannii*: Spotlight on the UDP-N-acetylmuramoyl-L-alanine-D-glutamate:meso-diaminopimelate ligase (MurE). *Journal of Biomolecular Structure and Dynamics*, 2024: 1-15.
54. Yang, Y., Wang, H., Zhou, H., Hu, Z., Shang, W., Rao, Y., Peng, H., Zheng, Y., Hu, Q., Zhang, R., Luo, H., and Rao, X. (2020). Protective effect of the golden staphyloxanthin biosynthesis pathway on *Staphylococcus aureus* under cold atmospheric plasma treatment. *Applied and Environmental Microbiology*, 86(3): e01998-19.
 55. Khan, M. A. S., Miah, M. I., Islam, Z., Afrin, S., Ahmed, M. F., and Rahman, S. R. (2023). Molecular docking and dynamics simulation study of medicinal fungi derived secondary metabolites as potential inhibitor for COVID-19 treatment. *Informatics in Medicine Unlocked*, 41(5): 101305.
 56. El-sayed, N. N. E., Al-otaibi, T. M., Alonazi, M., Masand, V. H., Barakat, A., Almarhoon, Z. M., and Bacha, A. Ben. (2021). Synthesis and characterization of some new Quinoxalin-2(1h)one and 2-methyl-3h-quinazolin-4-one derivatives targeting the onset and progression of CRC with SAR, molecular docking, and ADMET analyses. *Molecules*, 26: 3121.
 57. Almalki, A. J., Ibrahim, T. S., Elhady, S. S., Darwish, K. M., and Hegazy, W. A. H. (2022). Repurposing α -adrenoreceptor blockers as promising anti-virulence agents in gram-negative bacteria. *Antibiotics*, 11(2): 178.
 58. Anwar, S., Khan, S., Shamsi, A., Anjum, F., Shafie, A., Islam, A., Ahmad, F., and Hassan, M. I. (2021). Structure-based investigation of MARK4 inhibitory potential of Naringenin for therapeutic management of cancer and neurodegenerative diseases. *Journal of Cellular Biochemistry*, 122(10): 1445-1459.
 59. Karami, T. K., Hailu, S., Feng, S., Graham, R., & Gukasyan, H. J. (2022). Eyes on Lipinski's rule of five: A new "Rule of Thumb" for physicochemical design space of ophthalmic drugs. *Journal of Ocular Pharmacology and Therapeutics*, 38(1): 43-55.
 60. Mortadza, N. A., and Ngaini, Z. (2023). Microwave-assisted and conventional synthesis of halogenated coumarin-azo derivatives and structural-activity relationship study for antimicrobial potential. *Malaysian Journal of Analytical Sciences*, 27(2): 342-352.
 61. James, J. P., Ail, P. D., Crasta, L., Kamath, R. S., Shura, M. H., and T.J, S. (2023). *In silico* ADMET and molecular interaction profiles of phytochemicals from medicinal plants in Dakshina Kannada. *Journal of Health and Allied Sciences NU*, 14(2): 190-201.
 62. En-Nahli, F., Hajji, H., Ouabane, M., Ajana, M. A., Sekatte, C., Lakhlifi, T., and Bouachrine, M. (2023). ADMET profiling and molecular docking of pyrazole and pyrazolines derivatives as antimicrobial agents. *Arabian Journal of Chemistry*, 16(11): 105262.
 63. Abd Halim, A. N., Zikri, N. A. S., Ngaini, Z., Zamakshshari, N. H., Wei, Y. K., and Diosing, D. N. (2023c). Synthesis in silico and ADMET profile of triazinethione derivatives for their potential as anti-inflammatory agents. *Russian Journal of General Chemistry*, 93(11): 2889-2899.
 64. Pires, Blundell, T. L., and Ascher, D. B. (2015). pkCSM: Predicting small-molecule pharmacokinetic properties using graph-based signatures. *Journal of Medicinal Chemistry*, 58: 4066-4072.
 65. Kirishnamaline, G., Magdaline, J. D., Chithambarathanu, T., Aruldhas, D., and Anuf, A. R. (2021). Theoretical investigation of structure, anticancer activity and molecular docking of thiourea derivatives. *Journal of Molecular Structure*, 1225: 129118.
 66. Cosimelli, B., Lamartina, L., Lanza, C. Z., Spinelli, D., Spisani, R., and Vegna, F. (2003). Reaction of 3-bromo-2-nitrobenzo[b]thiophene with some ortho-substituted anilines: an analysis of the products of reaction and of their NMR and MS properties. *Tetrahedron*, 59(36): 7189-7201.
 67. Subi, E. B., Dhas, D. A., Balachandran, S., and Joe, I. H. (2022). Crystal growth, structural, vibrational, effects of hydrogen Bonding(C-H-O and C-HN), chemical reactivity, antimicrobial activity, inhibitory effects and molecular dynamic simulation of 4-Methoxy-N-(Nitrobenzylidene)-Aniline. *Polycyclic Aromatic Compounds*, 43(3): 2690-2744.